



Conditional deletion of *Bmp2* in cranial neural crest cells recapitulates Pierre Robin sequence in mice

Yixuan Chen¹ · Zhengsen Wang¹ · YiPing Chen^{1,2} · Yanding Zhang¹

Received: 11 June 2018 / Accepted: 22 September 2018
© Springer-Verlag GmbH Germany, part of Springer Nature 2018

Abstract

Bone morphogenetic protein (BMP) signaling plays a crucial role in the development of craniofacial organs. Mutations in numerous members of the BMP signaling pathway lead to several severe human syndromes, including Pierre Robin sequence (PRS) caused by heterozygous loss of *BMP2*. In this study, we generate mice carrying *Bmp2*-specific deletion in cranial neural crest cells using floxed *Bmp2* and *Wnt1-Cre* alleles to mimic PRS in humans. Mutant mice exhibit severe PRS with a significantly reduced size of craniofacial bones, cleft palate, malformed tongue and micrognathia. Palate clefting is caused by the undescended tongue that prevents palatal shelf elevation. However, the tongue in *Wnt1-Cre;Bmp2^{fl/fl}* mice does not exhibit altered rates of cell proliferation and apoptosis, suggesting contribution of extrinsic defects to the failure of tongue descent. Further studies revealed obvious reduction in cell proliferation and differentiation of osteogenic progenitors in the mandible of the mutants, attributing to the micrognathia phenotype. Our study illustrates the pathogenesis of PRS caused by *Bmp2* mutation, highlights the crucial role of BMP2 in the development of craniofacial bones and emphasizes precise coordination in the morphogenesis of palate, tongue and mandible during embryonic development.

Keywords *Bmp2* · Neural crest cells · Pierre Robin sequence · Cleft palate · Micrognathia

Introduction

In humans, newborn cleft palate due to a malpositioned tongue and underdeveloped mandible is clinically classified as Pierre Robin sequence (PRS) (Melkonimi et al. 2003; Rangeeth et al. 2011; Tan et al. 2013). In mice, mutations in genes involved in signaling pathways of TGF β , FGF and EGF such as *Prdm16*, *Tak1* and *Erk2* cause cleft palate resembling human PRS (Bjork et al. 2010; Parada et al. 2015; Song et al. 2013). While significant progress has been made recently, the pathogenesis of PRS is still elusive due to lack of relevant animal models.

Cleft palate is one of the most common congenital malformations in humans, with an incidence between 1/700 and 1/1000 (Koillinen et al. 2005). The etiology of cleft palate has been studied for decades. Many clefts are thought to be caused by a combination of genetic and environmental perturbations. Palatogenesis is a complex and precise process that leads to fusion of the primary palate with a bilateral pair of the secondary palatal shelves. The development of the secondary palate can be divided into five stages, including initiation, growth, elevation, contact and fusion. Although disruptions to any of these steps could result in cleft palate formation, approximately 90% of isolated cleft palate cases are caused by defective palatal elevation (Ferguson 1977). Palatal elevation is a step that turns the palatal shelves from the vertical position along the tongue to the horizontal position above the tongue. It is believed that palatal elevation is triggered by intrinsic forces in the palatal shelf itself and requires coordination with the growth and movement of surrounding craniofacial structures (Ferguson 1988). Many mouse models have been made to illustrate the mechanisms of failed or delayed palatal elevation (Alappat et al. 2005; Barrow and Capecchi 1999; Bjork et al. 2010; Casey et al. 2006; He et al. 2010a, b; Huang et al. 2008; Lan et al. 2004; Matsumura et al. 2011;

Electronic supplementary material The online version of this article (<https://doi.org/10.1007/s00441-018-2944-5>) contains supplementary material, which is available to authorized users.

✉ Yanding Zhang
ydzhang@fjnu.edu.cn

¹ Southern Center for Biomedical Research, Fujian Key Laboratory of Developmental and Neural Biology, College of Life Sciences, Fujian Normal University, Fuzhou 350108, China

² Department of Cell and Molecular Biology, Tulane University, New Orleans, LA 70118, USA

Rice et al. 2004; Xiong et al. 2009). Among these models, physical obstructions including a small mandible, abnormal palatal shelf-mandible fusion, or hindrance by the tongue appear to be major factors.

It is well documented that bone morphogenetic proteins (BMP) signaling plays significant roles in palatogenesis (Baek et al. 2011; Zhang et al. 2002). Clinical studies have provided evidence that BMP2 haploinsufficiency results in severe craniofacial defects including PRS in humans (Sahoo et al. 2011). In mice, *Bmp2* is expressed in the developing craniofacial region including cranial bones (Choi et al. 2005), palatal mesenchyme (He et al. 2010b), tongue (Kim et al. 2005) and mandibular bone (Wang et al. 2013). The spatiotemporal profile of *Bmp2* expression strongly implies a functional involvement of this gene in craniofacial development including palatogenesis.

Cranial neural crest (CNC) cells are a cell population that derives from the dorsal neural tube and migrates into the craniofacial region, including the secondary palate and branchial arches, providing additional embryonic connective tissue needed for craniofacial development. Many of the craniofacial skeletons develop from CNC-derived mesenchymal progenitor cells, which directly differentiate into osteoblasts via intramembranous ossification (Chai et al. 1998, 2000; Chai and Maxson 2006; Ramaesh and Bard 2003).

In this study, we disrupted the BMP2 signaling pathway in neural crest cells by generating *Bmp2* conditional knockout mice using the *Wnt1-Cre* allele. Mutant mice exhibit multiple craniofacial malformations including cleft palate, mimicking the symptoms of human PRS.

Material and methods

Animals

Bmp2^{fl/fl}, *Wnt1-Cre* and *R26R^{mTmG}* transgenic mice were obtained from the Jackson Laboratory and have been described previously (Danielian et al. 1998; Ma and Martin 2005; Muzumdar et al. 2007). To specifically inactivate *Bmp2* in the neural crest-derived mesenchyme, *Wnt1-Cre;Bmp2^{fl/+}* mice were crossed with *Bmp2^{fl/fl}* mice to generate *Wnt1-Cre;Bmp2^{fl/fl}* mice and were mated with *Bmp2^{fl/+};R26R^{mTmG}* mice to obtain *Wnt1-Cre;Bmp2^{fl/fl};R26R^{mTmG}* mice. Animals and procedures used in this study were approved by the Fujian Normal University Institutional Animal Care and Use Committee.

In vitro roller culture

E13.5 mouse embryos were collected and decapitated in sterile ice-cold PBS. Embryonic tails were subjected to DNA extraction for genotyping. The heads with removal

of the tongue and mandible were placed in a 20-ml glass bottle filled with 2 ml of DMEM supplemented with 20% fetal calf serum. The bottles were incubated at 37 °C and 5% CO₂ on a rotary apparatus rotating at a speed of 4 rpm in a vertical position for 24 h. Samples were then washed in PBS, fixed in 4% paraformaldehyde and processed for histological examination.

Organ culture of palates

For in vitro palate fusion assay, paired palatal shelves were carefully dissected from E13.5 *Wnt1-Cre;Bmp2^{fl/fl}* mutant and control embryos and placed on a filter paper in Trowell type organ culture, being oriented and juxtaposed with the MEE facing each other closely, as described previously (He et al. 2011). Samples were cultured in DMEM culture medium supplemented with 20% fetal calf serum and incubated at 37° and 5% CO₂ for 72 h. Medium was changed once after 48 h in culture. Samples were then collected for fixation and histological analysis.

Histology, in situ hybridization and immunohistochemistry

Mouse embryos were harvested from timed pregnant females and fixed in 4% paraformaldehyde solution at 4 °C overnight. Following dehydration through gradient ethanol, samples were embedded in paraffin and coronally sectioned at 8 μm. Slides were subjected to either hematoxylin/eosin staining for histological analysis or to in situ hybridization, as described previously (St Amand et al. 2000). For whole mount in situ hybridization, samples were dehydrated through gradient methanol after overnight fixation in 4% PFA and were subjected to in situ hybridization assay as described (Zhang et al. 1999). Antibodies used for immunohistochemistry staining include anti-Msx1 (R&D Systems, AF5045; 1:100), anti-Sox9 (Abcam, ab3697; 1:200), anti-Phospho-Smad1 (Ser463/465)/Smad5(Ser463/465)/Smad8(Ser426/428) (Millipore, AB3848; 1:100), anti-Ki67 (M3060; 1:200), anti-Sp7/Osterix (Abcam, ab22552; 1:100), anti-histone H3 (phosphor S10) (PHH3; Abcam, ab47297; 1:1000), anti-Caspase3 (Bioss, bs-0081R; 1:100) and anti-phospho-p38 MAPK (Thr180Tyr182) (Cell Signaling Technology, 4511s; 1:200).

Micro-computed tomography

Wild-type and *Wnt1-Cre;Bmp2^{fl/fl}* newborn mice were sacrificed and heads were fixed in 4% paraformaldehyde. The skulls were imaged using a microCT system (Scanco Medical, Bassersdorf, Switzerland).

Skeletal staining

Sacrificed P0 mice were eviscerated and skinned. Skeletons were stained with Alcian blue for demineralized cartilage and Alizarin Red for bone. Briefly, skinned mice were fixed in 100% ethanol for 2 days and then in acetone for 3 days. Samples were washed in water for 3 min and then stained for 5 days in a solution consisting of 1 vol 0.1% Alizarin Red S (in 95% ethanol), 1 vol 0.3% Alcian blue (in 70% ethanol), 1 vol 100% acetic acid and 17 vol ethanol, followed by 2% KOH for hydrolysis and gradient glycerol clearing.

Measurements

For mandible length measurement, mandibles were dissected carefully after skeletal staining and photographed using a Zeiss digital capture system with a digital caliper. The length of the mandible was measured from the most anterior to the end of the condyle. Ten samples were collected for measurement. For tongue height measurement, HE-stained coronal sections of E13.5 and E14.5 embryonic heads were photographed using an Olympus digital capture system with a digital caliper. Littermates of wild-type controls and mutant mice were processed in parallel for comparison. Sections at comparable levels along the anterior to the posterior axis were selected and the height of the tongue was measured from the bottom of the tongue to the most superior aspect of the mid-tongue epithelium along the midline. Three continuous sections at each level were measured. For volumetric analysis, consecutive 10- μ m sections along the anterior to posterior axis of the tongue were stained by Hematoxylin/Eosin staining and imaged using an Olympus digital capture system. Images were loaded into Amira 6.01 for 3D reconstruction and volumetric analyses. Statistical analysis of the measurements was performed using Excel and a paired Student's *t* test. Statistical significance was determined if $p < 0.05$.

Results

Gross phenotype of *Wnt1-Cre;Bmp2^{ff}* mice

It has been previously reported that microdeletions at 20p12.3 containing the *BMP2* allele lead to PRS in humans, suggesting that loss of *BMP2* function is one of the pathogenic factors (Sahoo et al. 2011). To create a mouse model for illustrating the underlying mechanisms of PRS caused by *BMP2* mutation, we generated *Wnt1-Cre;Bmp2^{ff}* mice with specific *Bmp2* loss of function in the neural crest cells-derived craniofacial structures. Results from in situ hybridization of *Bmp2* showed a significantly reduced *Bmp2* signal in craniofacial structures of *Wnt1-Cre;Bmp2^{ff}* mice, including palate, mandibular bone and Meckel's cartilage (Fig. S1). Mutant embryos died at birth

and exhibited multiple craniofacial malformations including micrognathia, cleft palate and maxillomandibular hypoplasia (Fig. 1). Compared with wild-type mice, *Wnt1-Cre;Bmp2^{ff}* mice had an abnormal head shape with a smaller and shorter jaw (Fig. 1 a, b) and complete cleft palate (Fig. 1 c, d). Lateral views of 3D reconstructions from microCT scans further confirmed severe craniofacial bone defects in mutant mice, including a ~40% reduction in the zygomatic volume and a ~10% reduction in the length of the mandibular bone with a missing coronoid process (Fig. 1 e, f, g, h, k). It is noteworthy that the defect in the proximal region of the mandible appeared relatively severe, while the distal region was mild (Fig. 1 g, h). In addition, skeleton preparations further revealed serious deformity in the maxilla of *Wnt1-Cre;Bmp2^{ff}* mice, including the palatine processes, the presphenoid bone and the sphenoid bone (Fig. 1 i, j).

Bmp2-deficient mice exhibit no intrinsic defects in the palatal shelves

It has been reported that at E12.5 and E13.5, *Bmp2* is expressed in the anterior palatal as well as in the nasal side palatal mesenchyme and the medial edge epithelium (MEE) region in the posterior palate (Fig. S1; He et al. 2010b). Our results showed that *Wnt1-Cre;Bmp2^{ff}* died of severe cleft palate defect at birth. To explain whether *Bmp2* is an intrinsic regulator of palatal shelf elevation and fusion, we examined and compared histology of the developing palatal shelves and surrounding structures in both mutant and wide-type embryos. Coronal sections of the E13.5 head revealed comparable morphology between control (Fig. 2 a–c) and mutant (Fig. 2 d–f) palatal shelves at the anterior, middle and posterior domains. However, while the palatal shelves of the controls have elevated to upon the tongue and were undergoing fusion at the midline at E14.5 (Fig. 2 g–i), the palatal shelves of the mutants remained in the vertical position on both sides of the heightened tongue, failing to elevate along the anterior-posterior axis (Fig. 2 j–l). At E16.5, the palatal shelves of controls have fused completely but the mutant palatal shelves were kept at the vertical position, exhibiting a phenotype of complete cleft palate (Fig. 2 m–r). Apart from the defect in palatal development, significantly, reduction in the size of Meckel's cartilage was observed in mutant embryos (Fig. 2 s, t), consistent with *Bmp2* expression in Meckel's cartilage as well as its role in skeletal development (Shu et al. 2011; Tsuji et al. 2006). Our results indicate that deletion of *Bmp2* in CNC-derived craniofacial mesenchyme leads to cleft palate formation due to failed palatal shelf elevation. Undescended tongue is a known major extrinsic obstruction that prevents the palatal shelf elevation. We measured the height of the tongue in both wild-type and mutant sections along the anterior to posterior axis. At E13.5, we did not observe a significant difference ($P > 0.05$) between controls and mutants (Fig. 2

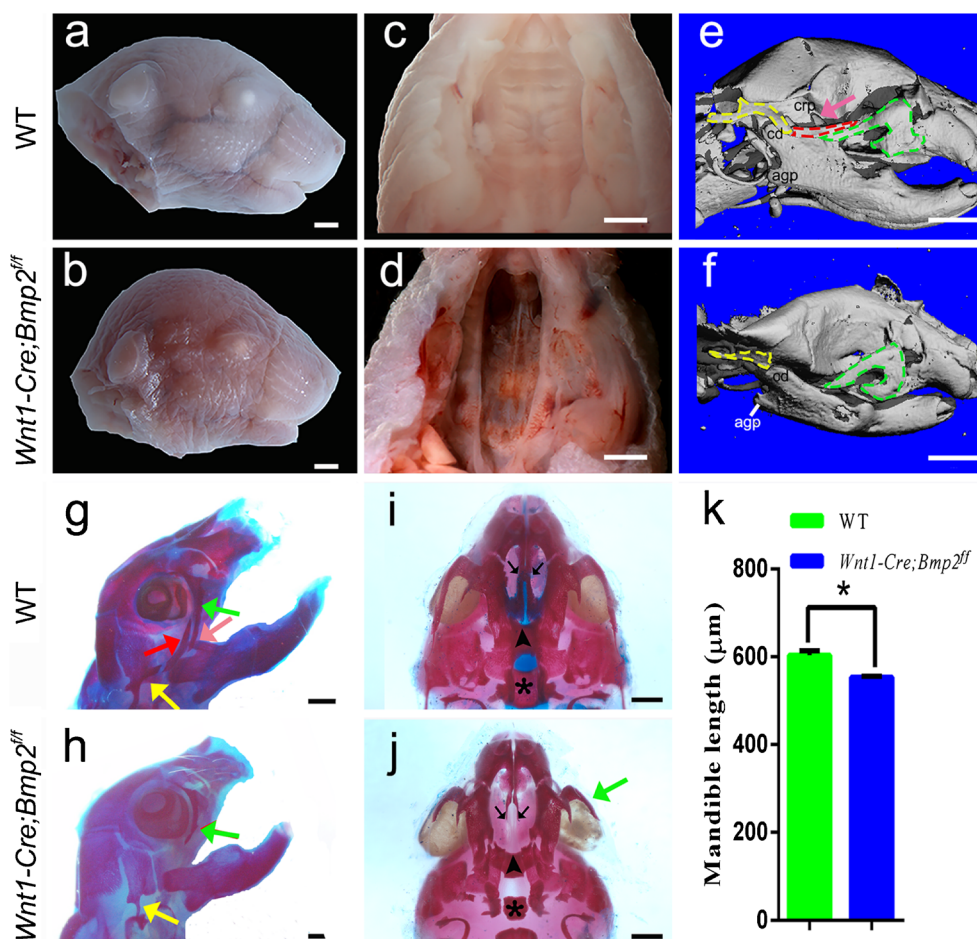


Fig. 1 Craniofacial defects of *Wnt1-Cre;Bmp2^{ff}* mutant mice. (a, b) Macroscopic lateral views of newborn wild-type and *Wnt1-Cre;Bmp2^{ff}* heads. (c, d) Macroscopic intraoral views of the palate of newborn wild-type and *Wnt1-Cre;Bmp2^{ff}*. (e, f) Lateral views of 3D reconstructions of newborn wild-type and *Wnt1-Cre;Bmp2^{ff}* heads from microCT scans. The zygomatic process of the maxilla (green dashed lines), the zygomatic bone (red dashed lines) and the zygomatic process of squamous (yellow dashed lines) are marked. Pink arrow in (e) points to the coronoid process of mandibular bone. (g–j) Skeletal staining of newborn head and

maxillary bone in controls and mutants. The zygomatic process of the maxilla (green arrow); the zygomatic bone (red arrow); the zygomatic process of squamous (yellow arrow). Pink arrow in (g) points to the coronoid process of mandibular bone; black arrows point to the palatine processes of the maxillary bone (i, j); black arrowheads point to the presphenoid bone and asterisks mark sphenoid bone (i, j); green arrow points to the zygomatic process of the maxilla (j). (k) Statistical analysis of the mandible length measurements. Crp coronoid process, cd condyle, agp angular process. * $P < 0.01$. Scale bars 1000 μm

u). However, the mutant tongue was obviously higher ($P < 0.005$) along the anterior-posterior axis than that of the wild type at E14.5 (Fig. 2 v). Meanwhile, we analyzed E13.5 and E14.5 tongue volumes of wild-type and *Bmp2* mutants and found no significant difference between them ($P > 0.05$) (Fig. 2 w).

The abovementioned results suggested that cleft palate in *Wnt1-Cre;Bmp2^{ff}* mice is not a consequence of an intrinsic defect but a secondary defect caused by the undescended tongue. To further confirm this idea, we performed in vitro roller culture and palate fusion assay to test if elevation and fusion of the palate could happen in the mutant mouse. Individual embryonic head of E13.5 embryos with the removal of the mandible and tongue was harvested and subjected to in vitro roller culture for 24 h and then processed for

histological examination. Paired palatal shelves were isolated from individual E13.5 embryo and subjected to organ culture for 72 h for palate fusion assay. As shown in Fig. 3, similar to the wild-type controls, the palatal shelves of mutants were able to elevate in roller culture (Fig. 3 a–d) and to fuse in organ culture (Fig. 3 e, f). These results demonstrated that the failure of palatal shelf elevation in embryo lacking *Bmp2* in CNC-derived mesenchyme is due to the steric hindrance of the higher tongue. *Bmp2* itself is not an intrinsic regulator of palatal shelf elevation and fusion.

Impaired CNC cell migration, proliferation and survival have been implicated in cleft palate formation (He et al. 2010b; He et al. 2008). Therefore, we set to examine if any of these events are impaired, contributing to the cleft palate defect in *Wnt1-Cre;Bmp2^{ff}* mice. By comparing the whole

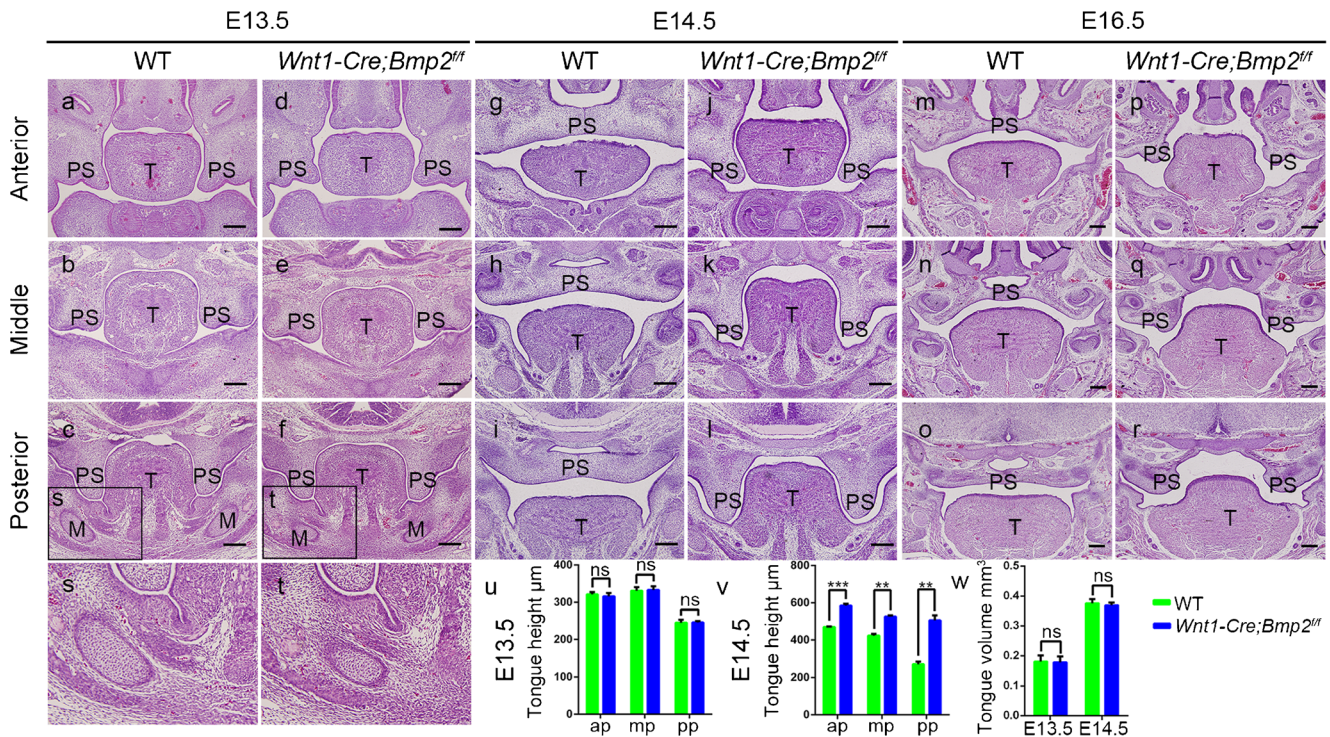


Fig. 2 Deletion of *Bmp2* in CNC cells leads to complete cleft palate due to failed palatal shelf elevation. (a–f) Histological sections show comparable morphology of wild-type (a–c) and mutant (d–f) palatal shelves at the anterior, middle and posterior domains at E13.5. (g–l) Histological sections show failed elevation of palatal shelves at E14.5 in *Wnt1-Cre;Bmp2^{ff}* mice (j–l) compared with stage-matched wild type (g–i). (m–r) At E16.5, the palatal shelves of controls fuse completely (m–o), but the mutant palate shelves are still kept at the vertical position (p–r). (s, t) Boxed areas in (c) and (f) are enlarged in (s) and (t). (u, v) Measurement of tongue height in both wild type and mutant along the anterior-posterior axis of E13.5 and E14.5. (w) Comparison of tongue volumes of wild type and mutant (wild type, *n* = 3; mutant, *n* = 3). NS not significant; *P* > 0.05; ***P* < 0.005; ****P* < 0.001. M Meckel’s cartilage, PS palatal shelves, T tongue, ap anterior palate, mp middle palate, pp posterior palate. Scale bars 200 µm

(s, t) Boxed areas in (c) and (f) are enlarged in (s) and (t). (u, v) Measurement of tongue height in both wild type and mutant along the anterior-posterior axis of E13.5 and E14.5. (w) Comparison of tongue volumes of wild type and mutant (wild type, *n* = 3; mutant, *n* = 3). NS not significant; *P* > 0.05; ***P* < 0.005; ****P* < 0.001. M Meckel’s cartilage, PS palatal shelves, T tongue, ap anterior palate, mp middle palate, pp posterior palate. Scale bars 200 µm

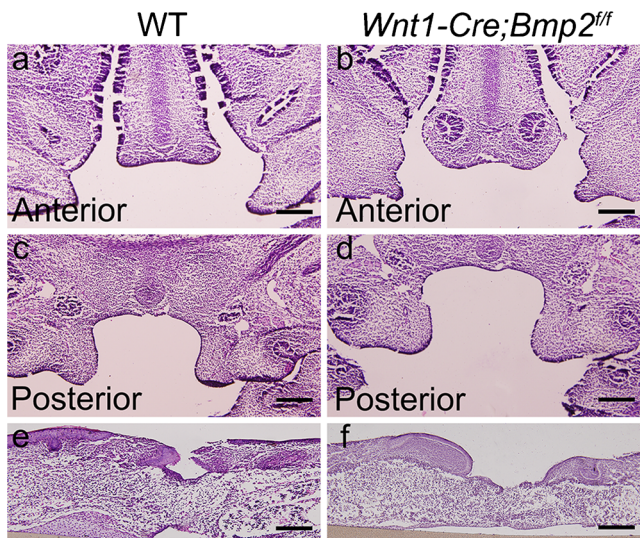


Fig. 3 Undescended tongue obstructs palatal shelf elevation. (a–d) Both wild-type controls and mutants show elevated palatal shelves after 24 h in organ culture. (e, f) In the in vitro palate fusion assay, mutant palatal shelves (f) fuse after 3-day culture, comparable to that seen in wide-type controls (e). Scale bars 200 µm

mount images of the first branch arch of *Wnt1-Cre;R26R^{mTmG}* controls and *Wnt1-Cre;Bmp2^{ff};R26R^{mTmG}* mice, we found no difference in timing of CNC cell migration and in tissue volume at E10.5 between them (Fig. 4 a, b), revealing that the availability of mesenchymal progenitors was not affected in the mutants. We then examined cell proliferation and apoptosis in the developing palatal shelves at E13.5 by immunostaining of Ki67 and caspase-3. We also found no obvious difference (*P* > 0.05) in the numbers of proliferating or apoptotic cells (Fig. 4 c–o). These results provide additional evidence that the cleft palate defect is not the consequence of intrinsic developmental defects of the palatal shelves of *Wnt1-Cre;Bmp2^{ff}* mice.

We next examined the expression of several selected genes that either show an overlapped expression pattern with *Bmp2* or play important roles during palatogenesis, including *Bmp7*, *Bmp4*, *Shh* and *Msx1*. We observed that the expression patterns of these genes remained unaltered in the mutant developing palate, as compared to controls (Fig. S2). It is known that both Smad-dependent and Smad-independent BMP signaling participate in palate development (He et al. 2010b; Xu et al. 2008). We therefore examined the activities of BMP/Smad signaling in the *Wnt1-Cre;Bmp2^{ff}* palatal shelves with

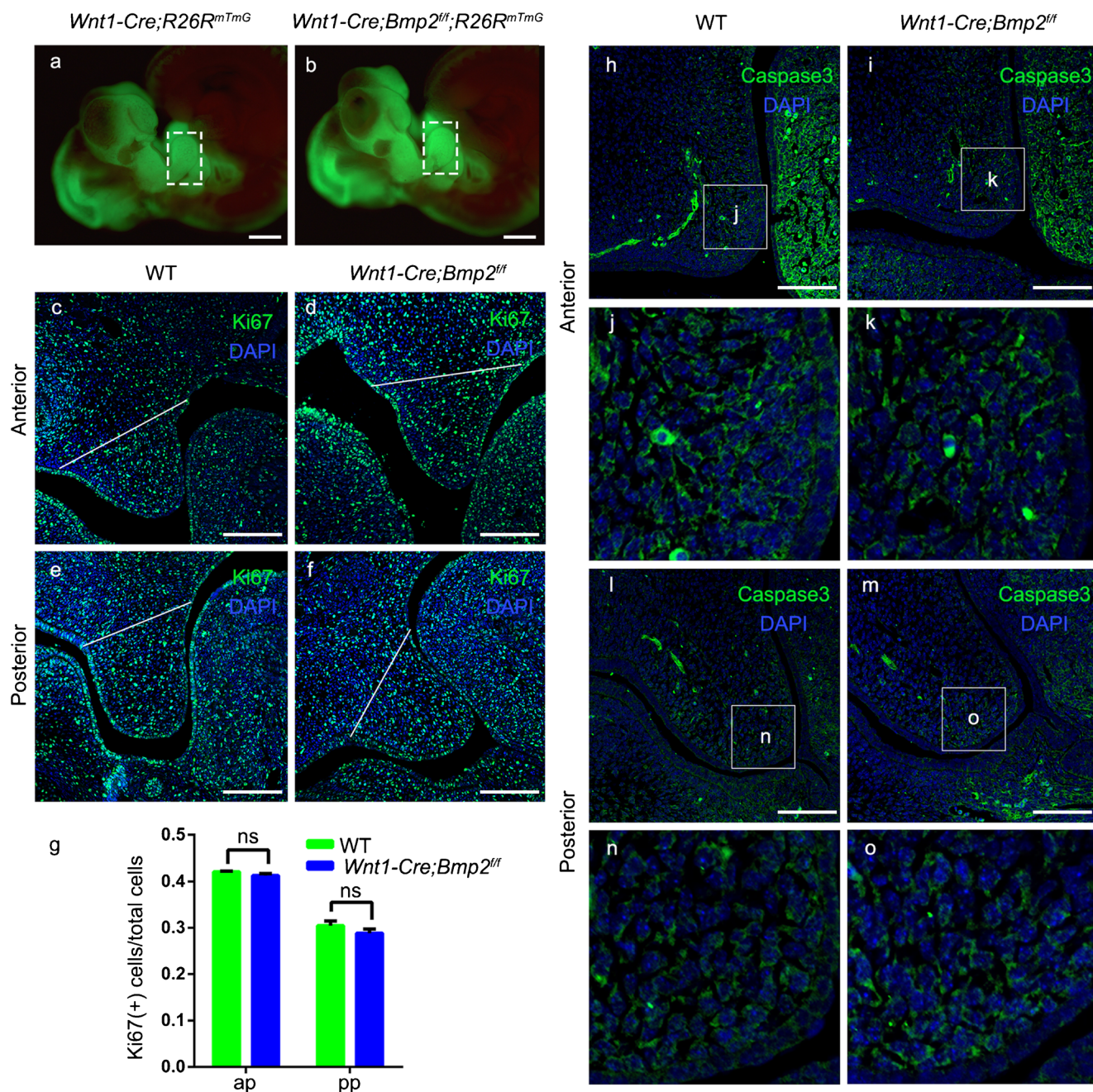


Fig. 4 Neural crest-derived cell migration, cell proliferation and apoptosis of palatal mesenchyme are unaffected in *Wnt1-Cre;Bmp2^{fl/fl}* mice. (a, b) Whole mount images of E10.5 *Wnt1-Cre;R26R^{mTmG}* and *Wnt1-Cre;Bmp2^{fl/fl};R26R^{mTmG}* embryos. The size of the first branchial arch (dashed box) appears comparable in both control and mutant. (c–f) Ki67 immunostaining (green) of wild type (c, e) and *Wnt1-Cre;Bmp2^{fl/fl}*

palates (d, f). White line demarcates the palatal shelf region for counting Ki67 positive cells. (g) Statistical data analysis shows cell proliferation rate is not affected. (h–o) Caspase immunostaining of wild type (h, j, l, n) and *Wnt1-Cre;Bmp2^{fl/fl}* palates (i, k, m, o). NS not significant. Scale bars 100 μ m

anti-phosphorylated Smad1/5/8 (pSmad1/5/8) antibody and found that, except in the future nasal side of the posterior palatal shelves where pSmad1/5/8 activity is almost abolished, the level and pattern of pSmad1/5/8 are unchanged in the mutant, as compared to controls (Fig. S3a–d). In addition, p38 MAPK signal, a Smad-independent BMP signaling pathway that is mainly active

in the epithelium regulating the fusion of the palate (Xu et al. 2008), is unaltered in the developing palate of *Wnt1-Cre;Bmp2^{fl/fl}* as well (Fig. S3e–h). Our results demonstrate that, although *Bmp2* is inactivated in CNC-derived mesenchymal tissues, the activities of BMP signaling in the mutant palate appear largely unaffected, most likely attributing to the functional redundancy by *Bmp4* and *Bmp7*.

It is documented that *Bmp2* is expressed only in the papilla epithelium of the developing tongue (Jung et al. 1999; Kim et al. 2005). Deletion of *Bmp2* in CNC cells would likely have no influence on the developing tongue. Indeed, examination of cell proliferation in the tongue using anti-histone H3 (phosphor S10) (PHH3), a marker of proliferation, reveals comparable cell proliferation rates ($P > 0.05$) between controls and mutants (Fig. 5 a–f). Next, we examined myogenic differentiation by analyzing the expression patterns of a heavy chain of myosin II, a differentiation marker of mature muscle fibers using MF20 antibody. No significant differences in the intensity and expression pattern of the signal were observed between control and mutant tongues at E13.5 and E14.5 (Fig. S4). We thus conclude that the elevated tongue in *Wnt1-Cre;Bmp2^{ff}* mice is not a consequence of increased cell proliferation or abnormal muscle patterning and organization. These results indicated that the tongue malformation in *Wnt1-Cre;Bmp2^{ff}* mice is a secondary defect caused by external forces.

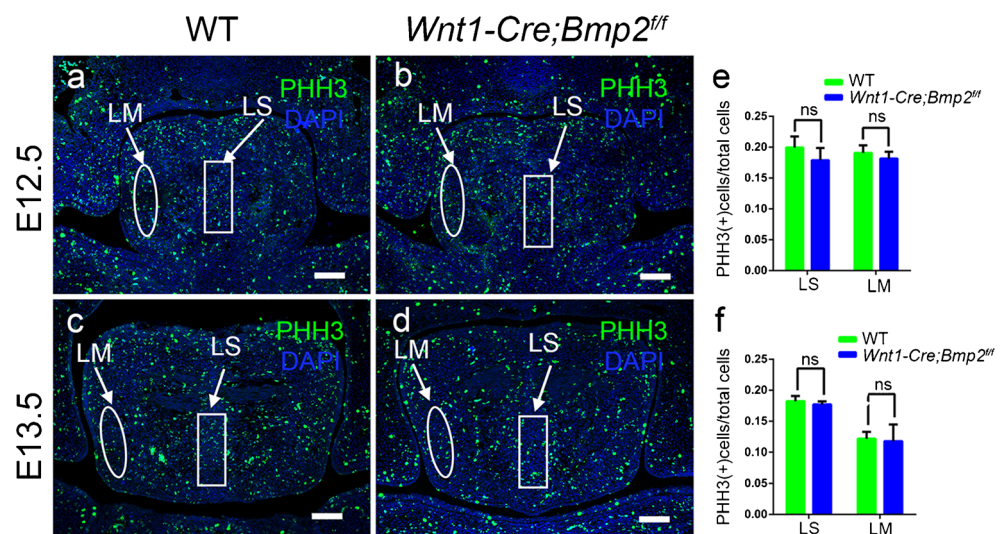
Mandibular osteogenic and chondrogenic differentiation are compromised in *Bmp2*-deficient mice

Bmp2 has been widely studied for its crucial biological functions during chondrogenic and osteogenic differentiation (Ducy and Karsenty 2000; Reddi 1997; Yang et al. 2013). *Bmp2* expression has been observed in mandibular primordium since E12.5 (Wang et al. 2013). Canonical and non-canonical BMP signaling have extensively recognized roles in bone formation (Fukuda et al. 2006; Greenblatt et al. 2010; Hoffmann et al. 2005; Retting et al. 2009; Wang et al. 2011). It is well established that tongue descending is tightly coordinated with outgrowth and expansion of the mandible. We thus extended our examinations

to the developing mandible. As shown in Fig. 6 (a–d), the mutant mandibular bone exhibits reduced pSmad1/5/8 and pp38 signals. In order to reveal the cause of mandibular hypoplasia, we examined cellular behaviors including cell proliferation and differentiation in the mandible from E12.5 to E16.5, the critical development period of the mandibular bone. We observed that the domain expressing Sp7, a molecular marker for osteogenic progenitors, is reduced throughout this period in *Wnt1-Cre;Bmp2^{ff}* mice compared to that in wild-type controls (Fig. 7 a–h), suggesting a reduced number of osteogenic progenitors at the beginning of mandibular ossification. Outgrowth of the coronoid process is apparently retarded (Fig. 1 g, h). *Bmp2* is also expressed in developing Meckel's cartilage (Wang et al. 2013), a transient structure derived from CNC cells. Since in *Wnt1-Cre;Bmp2^{ff}* mice, Meckel's cartilage also exhibited decreased pSmad1/5/8 activity (Fig. 6 a, b) and reduced size (Fig. 2 s, t), we, therefore, examined the expression of chondrogenesis marker Sox9. We found that both the expression area and the intensity of Sox9 are significantly reduced (Fig. 7 i–n).

Next, we tested if there was a decrease in cell proliferation in the mutant embryonic mandibular bone from E12.5 to E14.5 by comparing PHH3 positive cells in mutant Meckel's cartilage and mandibular bone with that in control ones. As shown in Fig. 8, the ratio of cell proliferation in the mandible of *Wnt1-Cre;Bmp2^{ff}* embryos was significantly reduced (Fig. 8 a–f, g, i, k), demonstrating that the decrease in proliferation rate occurred before the appearance of the morphological abnormality in the mandibular primordium. These results show that a decreased ratio of cell proliferation leads to reduction of osteogenic and chondrogenic progenitor cells and is responsible for the formation of smaller mandible in the mutants, which in turn prevents tongue descending and eventually leading to cleft palate formation.

Fig. 5 *Bmp2* deficiency has no impact on cell proliferation of the tongue. (a–d) PHH3 immunostaining of coronal sections of E12.5–E13.5 wild-type and *Wnt1-Cre;Bmp2^{ff}* tongues. (e, f) Quantification of proliferating cells in designated areas of the tongue in wild-type controls and mutants (wild type, $n = 3$; mutant, $n = 3$). LM lingual septum, LS longitudinal muscle, NS not significant. Scale bars 100 μ m



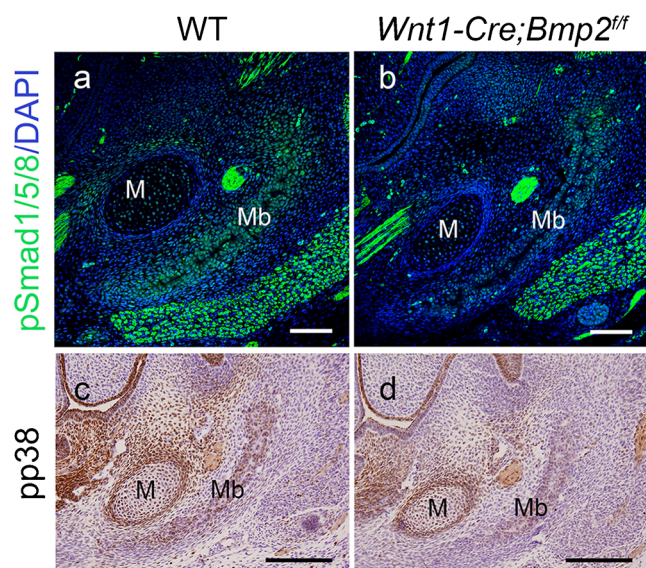


Fig. 6 *Bmp2* regulates mandibular osteogenic and chondrogenic development through both Smad-dependent and non-Smad-dependent BMP signaling. (a, b) pSmad1/5/8 immunostaining (green) on E13.5 wild-type (a) and *Wnt1-Cre;Bmp2^{ff}* (b) mandibles. Compared to wild-type controls, the mutant mandibular bone and Meckel's cartilage exhibit downregulated pSmad1/5/8 signals. (c, d) Immunohistochemical staining of pp38 on E13.5 wild-type and *Wnt1-Cre;Bmp2^{ff}* mandibles. As compared to wide-type control (c), the mutant mandibular bone shows decreased pp38 activity (d). Mb mandibular bone, M Meckel's cartilage. Scale bars 100 μ m

Discussion

Wnt1-Cre;Bmp2^{ff} mice exhibit phenotypes that mimic human PRS

It is well known that *Bmp2* is active in mesenchymal progenitors that are committed not only to the osteogenic but also to chondrogenic tissues. In this paper, we investigated the function of *Bmp2* in the development of CNC-derived craniofacial organs by deletion of *Bmp2* with a *Wnt1-Cre* allele. We found that inactivation of *Bmp2* in this cell lineage causes severe craniofacial malformations with typical PRS. In humans, the incidence of PRS is estimated to be about 1:8500 to 1:14000 (Tan et al. 2013). Patients with PRS have life-threatening obstructive apnea, feeding difficulties and ear infections during the neonatal period. PRS can only be truly diagnosed after birth. Several mouse models have been made to investigate the underlying mechanism of this congenital disease. Mutation in *Prdm16*, a downstream regulator mediating TGF β signaling, causes a secondary cleft palate due to a higher tongue and smaller mandible (Bjork et al. 2010). Deletion of *Tak1*, a key regulator of TGF β signaling, in CNC cells leads to cleft palate due to as well a secondary consequence by the steric hindrance of the elevated tongue (Song et al. 2013). Mice, bearing ablation of *Erk2*, an important mediator of the BMP, TGF β , FGF and EGF pathway, exhibit a similar phenotype (Parada et al. 2015). Here we

generated an animal model of *Wnt1-Cre;Bmp2^{ff}* mice that the 100% penetrance of the phenotype resembling the human PRS, providing an ideal model for further elucidating its pathogenesis and searching for precautionary measures and perhaps a more effective treatment.

Bmp2 is not an intrinsic regulator of palatal shelf elevation

Failed elevation of the palatal shelves is one of the direct causes of cleft palate in PRS. The elevation of palatal shelves is a complex process requiring synergy between the palate and other facial primordia (Ferguson 1988). Studies have been made to identify the intrinsic genetic factors that facilitate elevation in the palate shelf, including *Osr2* (Lan et al. 2004), *Gsk3 β* (He et al. 2010a) and *Golgb1* (Lan et al. 2016). Although *Bmp2* is expressed in the palate, our study shows it is not the intrinsic regulator guiding the elevation of the palatal shelf. *Bmp2*, *Bmp4* and *Bmp7*, functioning as mitogens during the development of craniofacial structures, are expressed in the epithelium and mesenchyme in a partially overlapping pattern in the anterior palate but not in the posterior palate (Fig. S2). Previous *in vivo* and *in vitro* experiments have demonstrated that both BMP2 and BMP4 alone induce cell proliferation in the anterior palatal mesenchyme but not in the posterior palate (Hilliard et al. 2005; Zhang et al. 2002). In *Wnt1-Cre;Bmp2^{ff}* mice, the cell proliferation rate and the activity of pSmad1/5/8 are unaltered in the anterior palate, suggesting that these BMP ligands have a functional redundancy and compensate for the absence of BMP2. Meanwhile, an unaltered cell proliferation ratio in the posterior palate is consistent with the previous study that neither BMP2 nor BMP4 are associated with cell proliferation in the posterior palate. Downregulation of pSmad1/5/8 in the posterior palate is likely attributed to the ablation of *Bmp2* since *Bmp7* is expressed only in the epithelium of the posterior portion. Together with our *in vitro* roller culture assay demonstrating that mutant palatal shelves elevate normally when the mandible is removed, our results strongly indicate that BMP2 is not an intrinsic factor for regulating palate elevation.

External forces by other facial primordia are the other indispensable element that drives palatal elevation. It is hypothesized that cranial base cartilage generates forces that are transmitted to the alar regions of the sphenoid to promote the elevation of palatal shelves (Brinkley and Vickerman 1978). However, it may not be the major reason in our animal model since the palate is able to elevate normally in *Wnt1-Cre;Bmp2^{ff}* mice with even severe sphenoid dysplasia when the mandible is removed. The roles of bone structure of the upper jaw in palatal development need to be further elucidated. A mandible with proper size and morphology provides space for the sinking of the tongue, thereby facilitating the

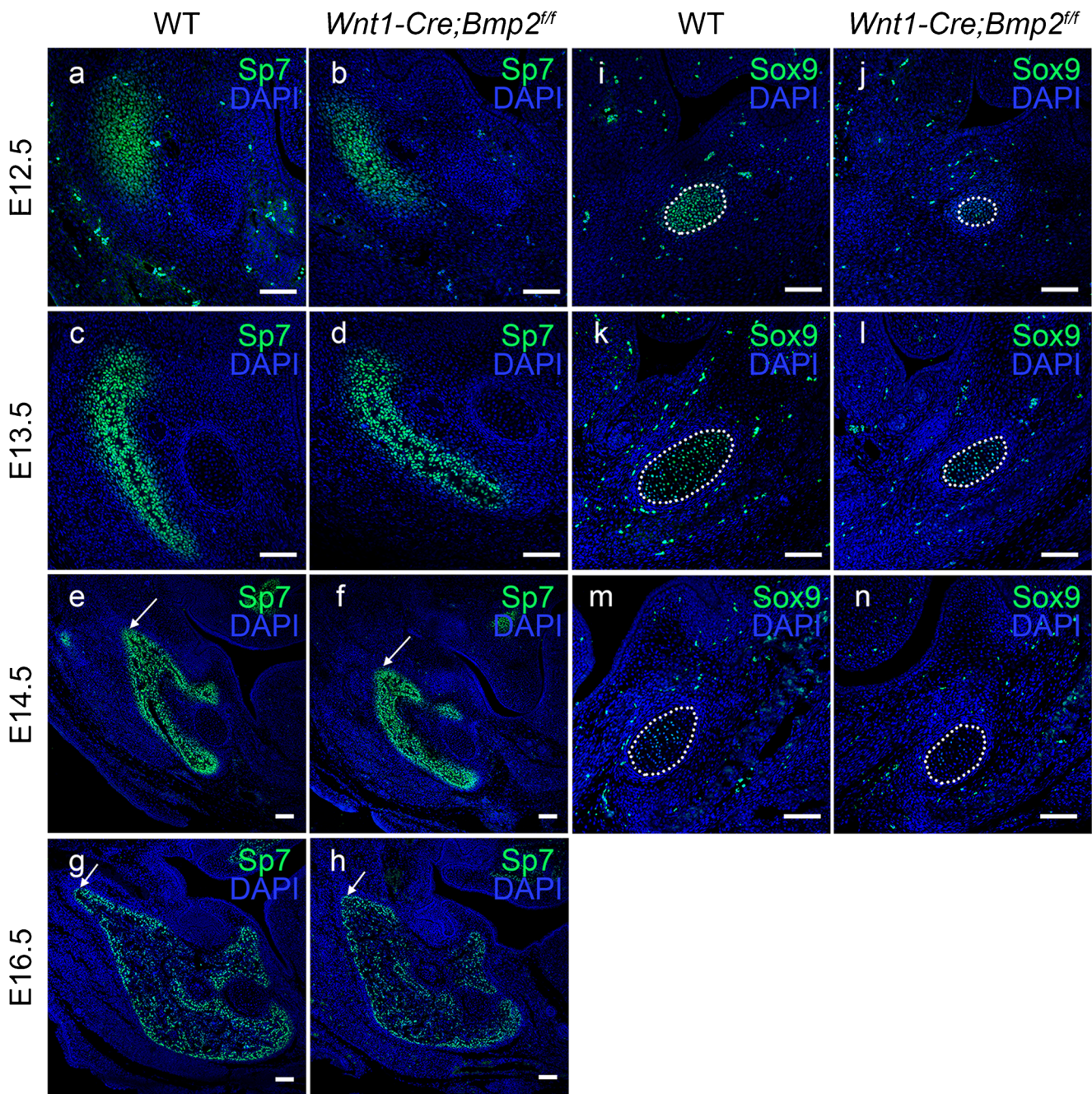


Fig. 7 Osteogenic and chondrogenic differentiations are compromised in the *Wnt1-Cre;Bmp2^{ff}* mandible. (a–h) Sp7 immunostaining of control and *Wnt1-Cre;Bmp2^{ff}* mandibles. The numbers of Sp7 positive cells in the forming mandibular bone of *Wnt1-Cre;Bmp2^{ff}* mutants appear reduced from E12.5 to E16.5. Arrows in (f) and (h) indicate the abnormal

morphology of Sp7 expressing domains in mutant embryos compared to that in wild-type controls at E14.5 and E16.5. (i–n) Sox9 immunostaining on control and *Wnt1-Cre;Bmp2^{ff}* Meckel's cartilages from E12.5 to E14.5 shows dramatically reduced Sox9 expression. White dot lines delineate Meckel's cartilages. Scale bars 100 μ m

repositioning of the palatal shelves from a vertical to horizontal position. The deformed mandible with reduced size in *Wnt1-Cre;Bmp2^{ff}* mice squeezes the space for the tongue to descend, resulting in a higher positioned tongue that hinders the elevation of the palatal shelves. Our study further demonstrates that structural defects are likely to cause severe craniofacial deformity, emphasizing the importance of the coordinated development of craniofacial structures.

***Bmp2* is a critical factor in craniofacial osteogenesis and chondrogenesis**

Bmp2 is required for determination of the chondrogenic cells in the cranial neural crest, including Meckel's cartilage. In mice, Meckel's cartilage is a transient support tissue that begins to develop at E11 and undergoes degeneration at E16.5 (Harada and Ishizeki 1998; Ramaesh and Bard 2003; Wang

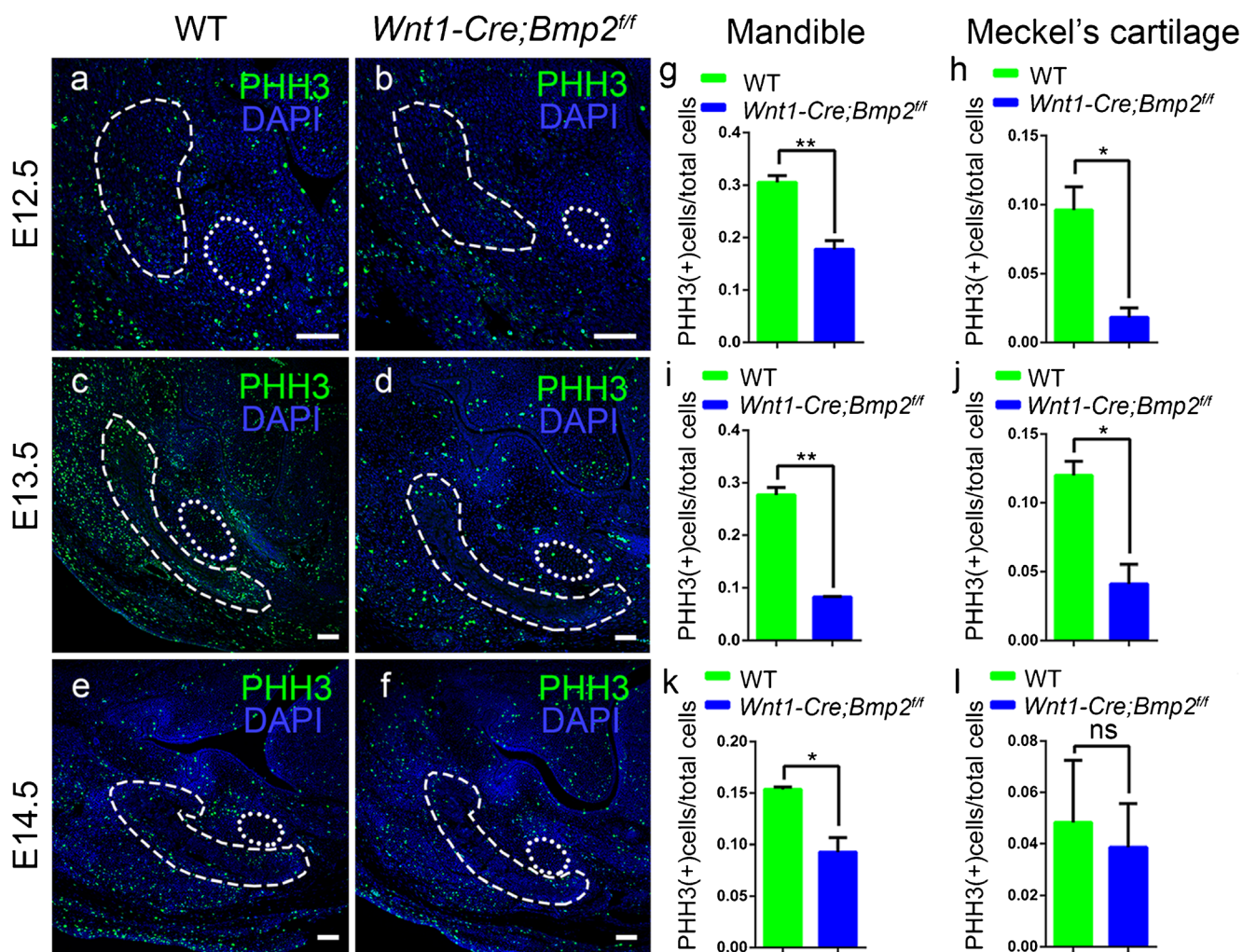


Fig. 8 Cell proliferation rate in both Meckel's cartilage and mandibular bone is remarkably decreased. (a–f) PHH3 immunostaining on control and *Wnt1-Cre;Bmp2^{ff}* mandible and Meckel's cartilage. (g–l) Quantification of proliferating cells of mandible and Meckel's cartilage

(wild type, $n = 5$; mutant, $n = 5$). * $P < 0.01$; ** $P < 0.005$; NS not significant. White dashed lines delineate the mandibular bones and white dot lines delineate Meckel's cartilages. Scale bars 100 μm

et al. 2013). *Noggin* mutant mice display enlargement and endochondral ossification of Meckel's cartilage and activation of *Bmpr1a* in chondrocyte-lineage resembles *Noggin*^{-/-} Meckel's cartilage phenotype (Wang et al. 2013), indicating that BMPs play an important role in chondrogenesis. In addition, *Prx-Cre;Bmp2^{ff}* mice have spontaneous fractures that do not resolve with time (Tsuji et al. 2006) and *Col2a1-Cre;Bmp2^{ff}* embryos exhibit a severe chondrodysplasia phenotype, suggesting that *Bmp2* is essential for chondrogenesis and other BMP ligands do not compensate for the role of *Bmp2* in chondrogenesis. This ideal is further supported by our results that though *Bmp7* is detected in Meckel's cartilage (Wang et al. 2013), ablation of *Bmp2* signal leads to a significant decrease in the proliferation and differentiation of chondrogenic cells, ultimately resulting in an dramatically reduced size of Meckel's cartilage.

Mandibular bone formation occurs through intramembranous ossification. Mandibular primordium is first

seen as a thin plate of condensed neural crest-derived mesenchymal cells at E12.5 and becomes distinguishable lateral to Meckel's cartilage at E13.5. Previous studies have shown that the BMP pathway participates in both endochondral and intramembranous ossification. *Bmp2* and *Bmp4* play differential roles in bone formation (Bonilla-Claudio et al. 2012; Chen et al. 2012). Spontaneous ablation of *Bmp2* and *Bmp4* by a transgenic *Prx-Cre* allele in limb bud mesenchyme exhibits a severe impairment of osteogenesis (Shu et al. 2011), while ablation of *Bmp4* alone in the same manner displays a normal limb development (Tsuji et al. 2008), suggesting that *Bmp2* but not *Bmp4*, is essential for bone formation. Moreover, *Wnt1-Cre;Bmp4^{ff}* mice exhibit enlarged frontal fontanelle and subtle mandibular defects, while *Wnt1-Cre;Bmp2^{ff};Bmp4^{ff}* mice have a significant decrease in most CNC-derived bones, further supporting that *Bmp2* has a greater effect on osteogenesis than *Bmp4* (Bonilla-Claudio et al. 2012). In this work, ablation of *Bmp2* in neural crest cells

leads to a hypogenesis in osteogenic proliferation and differentiation in the craniofacial region. PHH3 immunostaining shows the cell proliferation rate is severely reduced in the forming mandibular bone of *Wnt1-Cre;Bmp2^{fl/fl}* mice, suggesting that *Bmp2* is essential for the proliferation of osteoblasts. Decreased ratio of cell proliferation results in reduction of osteogenic progenitor cells revealed by an obvious decrement in the Sp7 expression domain. Subsequently, outgrowth of the mandible is apparently retarded resulting in the formation of micrognathia. Based on the expression pattern of *Bmp2* that is throughout the entire embryonic period in the developing mandibular bone, our data indicate that *Bmp2* stimulates osteoblastic progenitor proliferation from the outset when the mandibular primordium first appears and continues to until later stages of osteoblast differentiation. BMP signaling regulates mandible morphogenesis by promoting proliferation and differentiation of osteoblasts.

Clinical data show that a number of human syndromes are caused by mutations in diverse members of the BMP pathway. Most of these syndromes display various skeletal manifestations, including brachydactyly, sclerosteosis and craniofacial abnormalities (Chen et al. 2012). *Bmp2* is expressed in specific domains of the cranial bones, mandibular bone and Meckel's cartilage at early developmental stages. Our study, indeed, reveals that conditional deletion of *Bmp2* in neural crest cells results in severe craniofacial skeletal dysplasia, suggesting a requirement of BMP2 signaling in the differentiation of craniofacial bones.

Funding information This study was supported by grant from the National Natural Science Foundation of China (81870739), and by NIH grant (DE026482) to YPC.

Compliance with ethical standards

Animals and procedures used in this study were approved by the Fujian Normal University Institutional Animal Care and Use Committee.

Conflict of interest The authors declare that they have no conflict of interest.

References

Alappat SR, Zhang Z, Suzuki K, Zhang X, Liu H, Jiang R, Yamada G, Chen Y (2005) The cellular and molecular etiology of the cleft secondary palate in *Fgf10* mutant mice. *Dev Biol* 277:102–113

Baek JA, Lan Y, Liu H, Maltby KM, Mishina Y, Jiang R (2011) *Bmpr1a* signaling plays critical roles in palatal shelf growth and palatal bone formation. *Dev Biol* 350:520–531

Barrow JR, Capocchi MR (1999) Compensatory defects associated with mutations in *Hoxa1* restore normal palatogenesis to *Hoxa2* mutants. *Development* 126:5011–5026

Bjork BC, Turbe-Doan A, Prysak M, Herron BJ, Beier DR (2010) *Prdm16* is required for normal palatogenesis in mice. *Hum Mol Genet* 19:774–789

Bonilla-Claudio M, Wang J, Bai Y, Klysiak E, Selever J, Martin JF (2012) *Bmp* signaling regulates a dose-dependent transcriptional program to control facial skeletal development. *Development* 139:709–719

Brinkley LL, Vickerman MM (1978) The mechanical role of the cranial base in palatal shelf movement: an experimental re-examination. *J Embryol Exp Morphol* 48:93–100

Casey LM, Lan Y, Cho ES, Maltby KM, Gridley T, Jiang R (2006) *Jag2-Notch1* signaling regulates oral epithelial differentiation and palate development. *Dev Dyn* 235:1830–1844

Chai Y, Maxson RE Jr (2006) Recent advances in craniofacial morphogenesis. *Dev Dyn* 235:2353–2375

Chai Y, Bringas P Jr, Shuler C, Devaney E, Grosschedl R, Slavkin HC (1998) A mouse mandibular culture model permits the study of neural crest cell migration and tooth development. *Int J Dev Biol* 42:87–94

Chai Y, Jiang X, Ito Y, Bringas P, Han J, Rowitch DH, Soriano P, McMahon AP, Sucov HM (2000) Fate of the mammalian cranial neural crest during tooth and mandibular morphogenesis. *Development* 127:1671–1679

Chen G, Deng C, Li Y-P (2012) TGF- β and BMP signaling in osteoblast differentiation and bone formation. *Int J Biol Sci* 8:272–288

Choi KY, Kim HJ, Lee MH, Kwon TG, Nah HD, Furuichi T, Komori T, Nam SH, Kim YJ, Kim HJ, Ryoo HM (2005) *Runx2* regulates FGF2-induced *Bmp2* expression during cranial bone development. *Dev Dyn* 233:115–121

Danielian PS, Muccino D, Rowitch DH, Michael SK, McMahon AP (1998) Modification of gene activity in mouse embryos in utero by a tamoxifen-inducible form of Cre recombinase. *Curr Biol* 8:1323–1326

Ducy P, Karsenty G (2000) The family of bone morphogenetic proteins. *Kidney Int* 57:2207–2214

Ferguson MWJ (1977) The mechanism of palatal shelf elevation and the pathogenesis of cleft palate. *Virchows Arch A Pathol Anat Histol* 375:97–113

Ferguson MWJ (1988) Palate development. *Development* 103:41

Fukuda T, Scott G, Komatsu Y, Araya R, Kawano M, Ray MK, Yamada M, Mishina Y (2006) Generation of a mouse with conditionally activated signaling through the BMP receptor, *ALK2*. *Genesis* 44:159–167

Greenblatt MB, Shim JH, Zou W, Sitara D, Schweitzer M, Hu D, Lotinun S, Sano Y, Baron R, Park JM, Arthur S, Xie M, Schneider MD, Zhai B, Gygi S, Davis R, Glimcher LH (2010) The p38 MAPK pathway is essential for skeletogenesis and bone homeostasis in mice. *J Clin Invest* 120:2457–2473

Harada Y, Ishizeki K (1998) Evidence for transformation of chondrocytes and site-specific resorption during the degradation of Meckel's cartilage. *Anat Embryol (Berl)* 197:439–450

He F, Xiong W, Yu X, Espinoza-Lewis R, Liu C, Gu S, Nishita M, Suzuki K, Yamada G, Minami Y, Chen Y (2008) *Wnt5a* regulates directional cell migration and cell proliferation via *Ror2*-mediated noncanonical pathway in mammalian palate development. *Development* 135:3871–3879

He F, Popkie AP, Xiong W, Li L, Wang Y, Phiel CJ, Chen Y (2010a) *Gsk3 β* is required in the epithelium for palatal elevation in mice. *Dev Dyn* 239:3235–3246

He F, Xiong W, Wang Y, Matsui M, Yu X, Chai Y, Klingensmith J, Chen Y (2010b) Modulation of BMP signaling by *Noggin* is required for the maintenance of palatal epithelial integrity during palatogenesis. *Dev Biol* 347:109–121

He F, Xiong W, Wang Y, Li L, Liu C, Yamagami T, Taketo MM, Zhou C, Chen Y (2011) Epithelial *Wnt/beta-catenin* signaling regulates palatal shelf fusion through regulation of *Tgfbeta3* expression. *Dev Biol* 350:511–519

Hilliard SA, Yu L, Gu S, Zhang Z, Chen YP (2005) Regional regulation of palatal growth and patterning along the anterior–posterior axis in mice. *J Anat* 207:655–667

- Hoffmann A, Preobrazhenska O, Wodarczyk C, Medler Y, Winkel A, Shahab S, Huylebroeck D, Gross G, Verschueren K (2005) Transforming growth factor-beta-activated kinase-1 (TAK1), a MAP3K, interacts with Smad proteins and interferes with osteogenesis in murine mesenchymal progenitors. *J Biol Chem* 280:27271–27283
- Huang X, Goudy SL, Ketova T, Litingtung Y, Chiang C (2008) Gli3-deficient mice exhibit cleft palate associated with abnormal tongue development. *Dev Dyn* 237:3079–3087
- Jung HS, Oropeza V, Thesleff I (1999) Shh, Bmp-2, Bmp-4 and Fgf-8 are associated with initiation and patterning of mouse tongue papillae. *Mech Dev* 81:179–182
- Kim JY, Cho SW, Lee MJ, Hwang HJ, Lee JM, Lee SI, Muramatsu T, Shimono M, Jung HS (2005) Inhibition of connexin 43 alters Shh and Bmp-2 expression patterns in embryonic mouse tongue. *Cell Tissue Res* 320:409–415
- Koillinen H, Lahermo P, Rautio J, Hukki J, Peyrard-Janvid M, Kere J (2005) A genome-wide scan of non-syndromic cleft palate only (CPO) in Finnish multiplex families. *J Med Genet* 42:177–184
- Lan Y, Oviatt CE, Cho ES, Maltby KM, Wang Q, Jiang R (2004) Odd-skipped related 2 (Osr2) encodes a key intrinsic regulator of secondary palate growth and morphogenesis. *Development* 131:3207–3216
- Lan Y, Zhang N, Liu H, Xu J, Jiang R (2016) Golgb1 regulates protein glycosylation and is crucial for mammalian palate development. *Development* 143:2344–2355
- Ma L, Martin JF (2005) Generation of a Bmp2 conditional null allele. *Genesis* 42:203–206
- Matsumura K, Taketomi T, Yoshizaki K, Arai S, Sanui T, Yoshiga D, Yoshimura A, Nakamura S (2011) Sprouty2 controls proliferation of palate mesenchymal cells via fibroblast growth factor signaling. *Biochem Biophys Res Commun* 404:1076–1082
- Melkoniemi M, Koillinen H, Mannikko M, Warman ML, Pihlajamaa T, Kaariainen H, Rautio J, Hukki J, Stofko JA, Cisneros GJ, Krakow D, Cohn DH, Kere J, Ala-Kokko L (2003) Collagen XI sequence variations in nonsyndromic cleft palate, Robin sequence and micrognathia. *Eur J Hum Genet* 11:265–270
- Muzumdar MD, Tasic B, Miyamichi K, Li L, Luo L (2007) A global double-fluorescent Cre reporter mouse. *Genesis* 45:593–605
- Parada C, Han D, Grimaldi A, Sarrion P, Park SS, Pelikan R, Sanchez-Lara PA, Chai Y (2015) Disruption of the ERK/MAPK pathway in neural crest cells as a potential cause of Pierre Robin sequence. *Development* 142:3734–3745
- Ramaesh T, Bard JB (2003) The growth and morphogenesis of the early mouse mandible: a quantitative analysis. *J Anat* 203:213–222
- Rangeeth BN, Moses J, Reddy NV (2011) Pierre robin sequence and the pediatric dentist. *Contemp Clin Dent* 2:222–225
- Reddi AH (1997) Bone morphogenetic proteins: an unconventional approach to isolation of first mammalian morphogens. *Cytokine Growth Factor Rev* 8:11–20
- Retting K, Song B, Yoon B, Lyons K (2009) BMP canonical Smad signaling through Smad1 and Smad5 is required for endochondral bone formation. *Development* 136:1093–1104
- Rice R, Spencer-Dene B, Connor EC, Gritli-Linde A, McMahon AP, Dickson C, Thesleff I, Rice DP (2004) Disruption of Fgf10/Fgfr2b-coordinated epithelial-mesenchymal interactions causes cleft palate. *J Clin Invest* 113:1692–1700
- Sahoo T, Theisen A, Sanchez-Lara PA, Marble M, Schweitzer DN, Torchia BS, Lamb AN, Bejjani BA, Shaffer LG, Lacassie Y (2011) Microdeletion 20p12.3 involving BMP2 contributes to syndromic forms of cleft palate. *Am J Med Genet A* 155A:1646–1653
- Shu B, Zhang M, Xie R, Wang M, Jin H, Hou W, Tang D, Harris SE, Mishina Y, O'Keefe RJ, Hilton MJ, Wang Y, Chen D (2011) BMP2, but not BMP4, is crucial for chondrocyte proliferation and maturation during endochondral bone development. *J Cell Sci* 124:3428–3440
- Song Z, Liu C, Iwata J, Gu S, Suzuki A, Sun C, He W, Shu R, Li L, Chai Y, Chen Y (2013) Mice with Tak1 deficiency in neural crest lineage exhibit cleft palate associated with abnormal tongue development. *J Biol Chem* 288:10440–10450
- St Amand TR, Zhang Y, Semina EV, Zhao X, Hu Y, Nguyen L, Murray JC, Chen Y (2000) Antagonistic signals between BMP4 and FGF8 define the expression of Pitx1 and Pitx2 in mouse tooth-forming anlage. *Dev Biol* 217:323–332
- Tan TY, Kilpatrick N, Farlie PG (2013) Developmental and genetic perspectives on Pierre Robin sequence. *Am J Med Genet C Semin Med Genet* 163C:295–305
- Tsuji K, Bandyopadhyay A, Harfe BD, Cox K, Kakar S, Gerstenfeld L, Einhorn T, Tabin CJ, Rosen V (2006) BMP2 activity, although dispensable for bone formation, is required for the initiation of fracture healing. *Nat Genet* 38:1424–1429
- Tsuji K, Cox K, Bandyopadhyay A, Harfe BD, Tabin CJ, Rosen V (2008) BMP4 is dispensable for skeletogenesis and fracture-healing in the limb. *J Bone Joint Surg Am* 90(Suppl 1):14–18
- Wang M, Jin H, Tang D, Huang S, Zuscik MJ, Chen D (2011) Smad1 plays an essential role in bone development and postnatal bone formation. *Osteoarthr Cartil* 19:751–762
- Wang Y, Zheng Y, Chen D, Chen Y (2013) Enhanced BMP signaling prevents degeneration and leads to endochondral ossification of Meckel's cartilage in mice. *Dev Biol* 381:301–311
- Xiong W, He F, Morikawa Y, Yu X, Zhang Z, Lan Y, Jiang R, Cserjesi P, Chen Y (2009) Hand2 is required in the epithelium for palatogenesis in mice. *Dev Biol* 330:131–141
- Xu X, Han J, Ito Y, Bringas P Jr, Deng C, Chai Y (2008) Ectodermal Smad4 and p38 MAPK are functionally redundant in mediating TGF-beta/BMP signaling during tooth and palate development. *Dev Cell* 15:322–329
- Yang W, Guo D, Harris MA, Cui Y, Gluhak-Heinrich J, Wu J, Chen XD, Skinner C, Nyman JS, Edwards JR, Mundy GR, Lichtler A, Kream BE, Rowe DW, Kalajzic I, David V, Quarles DL, Villareal D, Scott G, Ray M, Liu S, Martin JF, Mishina Y, Harris SE (2013) Bmp2 in osteoblasts of periosteum and trabecular bone links bone formation to vascularization and mesenchymal stem cells. *J Cell Sci* 126:4085–4098
- Zhang Y, Zhao X, Hu Y, St Amand T, Zhang M, Ramamurthy R, Qiu M, Chen Y (1999) Msx1 is required for the induction of patched by sonic hedgehog in the mammalian tooth germ. *Dev Dyn* 215:45–53
- Zhang Z, Song Y, Zhao X, Zhang X, Fermin C, Chen Y (2002) Rescue of cleft palate in Msx1-deficient mice by transgenic Bmp4 reveals a network of BMP and Shh signaling in the regulation of mammalian palatogenesis. *Development* 129:4135–4146